Montmorillonite for Adsorption and Catalytic Elimination of Pollutants from Wastewater: A State-of-the-Arts Review

Zakariyya Uba Zango [1,2,*], Abdurrahman Garba [1], Zaharaddeen Nasiru Garba [3], Muttaqa Uba Zango [4], Fahad Usman [2] and Jun-Wei Lim [5,6,*]

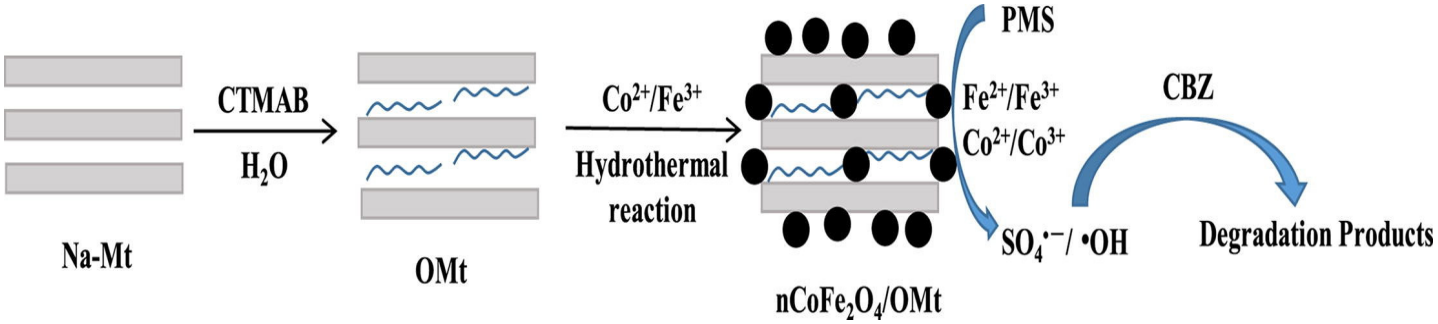

Figure S1. Synthesis of $nCoFe_2O_4$/MMT composite and its mechanism for carbamazepine (CBZ) photocatalytic degradation [1].

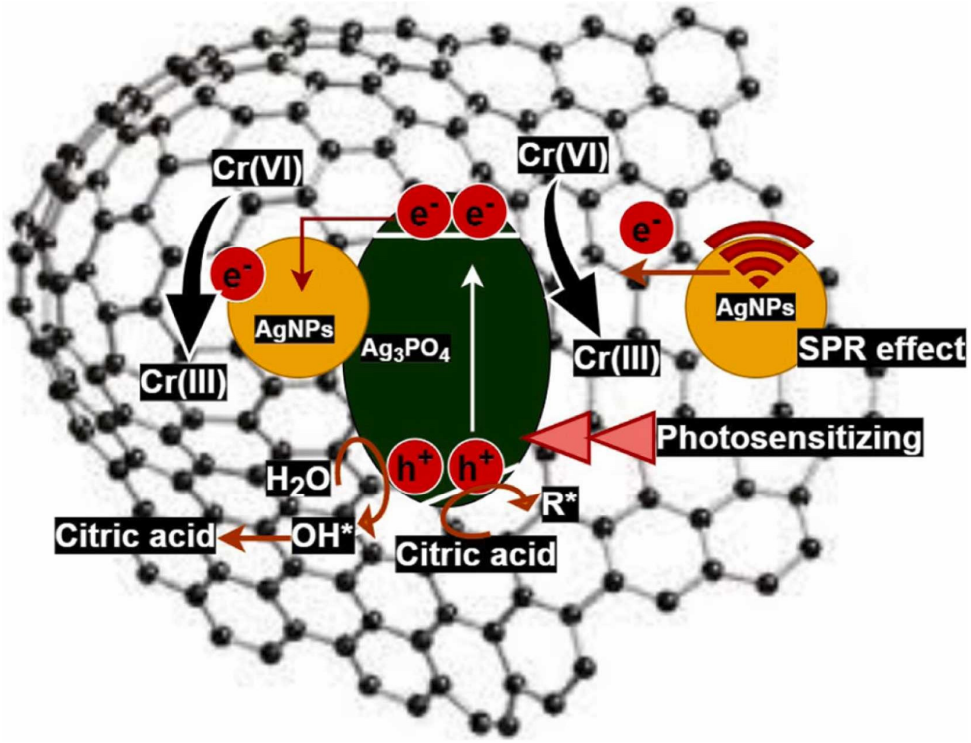

Figure S2. Mechanism for Cr (VI) photocatalytic degradation by MMT-Ag_3PO_4 composites [2].

Table S1. Compilation of various MMT composites as photocatalyst for dyes degradation.

Adsorbent	**Pollutant**	**Photocatalytic parameters**				Remark	**Ref**
		Catalyst weight (mg)	Concentration (mg/L)	Light source	Irradiation time		
MoS_2-MMT	MO	10	20	Visible light	90 min	The MoS_2 is the driving for the photocatalytic degradation, while the MMT nanosheet provided the abundant adsorption sites for the dye molecules	[3]
BiOCl-MMT	RhB OG	15	40	Mercury lamp	60 min	The catalyst inhibits charge recombination and exhibits higher degradation efficiency of the dyes due to the good photocurrent intensity of BiOCl.	[4]
Fe-MMT	CV	150	60	Solar lamp	240 min	Fe^{3+} helps on the generation of OH· radicals while the MMT adsorbed the dye for faster degradation.	[5]
Fe/Cu-MMT	RhB	150	100	Visible light	90 min	MMT provides more adsorption sites on the surface of the catalyst which improved OH radical production by the H_2O_2	[6]
MnO_2 nanosheet@MMT	MB	150	50	Visible light	60 min	MMT adsorbed the dye, while the MnO_2 produces free radicals that attack the dye for the photocatalytic degradation.	[7]

K10-APTES-3Gly-Fe MMT	CR MO MB	66	24.5	UV pen lamp	60 min	Rapid decomposition of the dyes was achieved, with CR having the least degradation due to its higher molecular weight.	[8]
BiOBr/MMT	RhB	50	40	Xenon lamp	120 min	The contact between BiOBr and Na-MMT resulted in lower photoelectrons recombination and good photocatalytic activity of the catalyst.	[9]
ZnO/MMT	DR54	62.5	40	UV light	60 min	ZnO immobilization on MMT leads to increase in surface area of the catalyst which resulted in more generation of h^+ that attack the dye.	[10]
Bi-doped TiO_2/MMT	RhB	50	10	Iodine tungsten lamp	210 min	MMT improved the adsorption of photons and RhB molecules onto the composite, achieving the degradation efficiency of 90.60%.	[11]
Cu/Pd-Ti-MMT	MB	6	200	Visible light	20 min	The catalytic degradation was aided by the Cu and Pd, and better efficiency was achieved at higher catalyst dosage.	[12]
Ag loaded B_2O_3/MMT	RhB	100	10	Visible light	240 min	Increasing the catalyst dosage improve the photocatalytic activity due to accessibility of more active sites, achieving over 90% degradation within 60 mins.	[13]
TiO_2-MMT	BB3	100	10	Ultrasonic power	90 min	TiO_2 negatively charged surface promotes radicals' production which attack the cationic dye.	[14]

TiO_2-MMT	RhB	150	10	Xenon lamp	120 min	MMT negatively charged surface acted as a carrier for transporting the photogenerated electron.	[15]
G-Fe-MMT	RB19	400	75	UV light	100 min	The catalyst exhibited higher solar absorption and generated more OH· radicals for the degradation of the dye.	[16]
γ-Fe_2O_3/MMT	RhB	-	10	Xenon lamp	60 min	Degradation efficiency of 96% was achieved, attributed to the higher adsorption capacity of the dye by the MMT.	[17]
Ni-TiO_2/CMMT	RO84	300	30	Tungsten lamp	120	TiO_2-Ni significantly reduced the bandgap of the catalyst and activated the visible light irradiation.	[18]
ZnO/MMT	MB	500	60	UV lamp	190 min	The ZnO/MMT achieved lower bandgap of 3.20 eV, thus achieved complete degradation of MB within 120 min.	[19]
MMT@MoS_2/CdS	RhB	100	20	Xenon lamp	45 min	MMT is the key. Factor for the adsorption of the dye while the MoS_2/CdS generates the electrons and holes for photodegradation.	[20]

Table S2. Compilation of various MMT composites as photocatalyst for pharmaceuticals and phenols degradation.

Catalyst	**Pollutant**	**Photocatalytic parameters**				**Remark**	**Ref**
		Catalyst weight (mg)	Concentration (mg/L)	Light source	Irradiation time		
Ag loaded B_2O_3/MMT	TC	100	20	Visible light	240 min	The photodegradation of RhB was favoured at lower of pH of 3 – 5, achieving 90 degradations within 60 mins.	[13]
MCC-MT-MB	TC	10	50	Red light	60 min	Degradation efficiency of TC increased with MB dosage due to the production of MB^* species which activate the photocatalyst.	[21]
Fe^{3+}-MMT	2,4-DNP	150	2	Solar simulator lamp	350 min	Replacement reaction takes place between Fe^{3+} and Na^+ of the MMT, leading to the generation of more OH radical that attacks the pollutant.	[22]
Ti-pillared MMT	TMP	-	25	UV light	240	MMT helps in the TiO_2 dispersion in the pillar, while Cr^{3+} and Fe^{3+} lowered the bandgap of the catalyst.	[23]
Fe_2O_3/MMT/PS	ENR	100	30	Visible light	60	MMT enhanced the adsorption of the ENR and PS generated the sulfate radicals that attack the pollutant.	[24]

$nCoFe_2O_4$-MMT	CBZ	400	5	Visible light	60	Increasing the dosage of the catalyst resulted in the increased number of active sites and provided more SO_4· and OH· radicals that initiated the degradation	[1]
SWy-2-MMT	DNOC PNP	500	200	Visible light	60	The OH· generation was induced by the electrolytes while the MMT provided sufficient surface area for the adsorption of the pollutants	[25]
SnO_2-MMT	TMP SMX	-	10	Solar light	-	SnO_2 promoted photoelectrons generation upon exposure to UV light, whereas the MMT provided sufficient sites for trapping the pollutants molecules.	[26]
$TiCl_4$-MMT	4-NP	300	15	UV light	220 min	Degradation efficiency of 97% was achieved due to the surface area enhancement and photoelectrons generation upon TiO_2 incorporation into the MMT.	[27]

References

1. Wu, J.; Cagnetta, G.; Wang, B.; Cui, Y.; Deng, S.; Wang, Y.; Huang, J.; Yu, G. Efficient degradation of carbamazepine by organo-montmorillonite supported nCoFe2O4-activated peroxymonosulfate process. *Chem. Eng. J.* **2019**, *368*, 824–836, doi:10.1016/j.cej.2019.02.137.

2. Abderrahim, N.; Djellabi, R.; Amor, H. Ben; Fellah, I.; Giordana, A.; Cerrato, G.; Di Michele, A.; Bianchi, C.L. Sustainable purification of phosphoric acid contaminated with Cr(VI) by Ag/Ag3PO4coated activated carbon/montmorillonite under UV and solar light: Materials design and photocatalytic mechanism. *J. Environ. Chem. Eng.* **2022**, *10*, doi:10.1016/j.jece.2022.107870.

3. Zhang, J.; Liu, T.; Fu, L.; Ye, G. Synthesis of nanosized ultrathin MoS2 on montmorillonite nanosheets by CVD method. *Chem. Phys. Lett.* **2021**, *781*, 138972, doi:10.1016/j.cplett.2021.138972.

4. Xu, C.; Gu, F.L.; Wu, H. BiOCl-montmorillonite as a photocatalyst for highly efficient removal of Rhodamine B and Orange G: Importance of the acidity and dissolved oxygen. *Appl. Clay Sci.* **2017**, *147*, 28–35, doi:10.1016/j.clay.2017.07.025.

5. Guz, L.; Curutchet, G.; Sanchez, R.M.T.; Candal, R. Adsorption of crystal violet on montmorillonite (or iron modified montmorillonite) followed by degradation through Fenton or photo-Fenton type reactions. *J. Environ. Chem. Eng.* **2014**, *2*, 2344–2351, doi:10.1016/j.jece.2014.02.007.

6. Zhang, X.; Guo, Y.; Shi, S.; Liu, E.; Li, T.; Wei, S. Efficient and stable iron-copper montmorillonite heterogeneous Fenton catalyst for removing Rhodamine B. *Chem. Phys. Lett.* **2021**, *776*, 138673, doi:10.1016/j.cplett.2021.138673.

7. He, Y.; Jiang, D. Bin; Chen, J.; Jiang, D.Y.; Xin, Y. Synthesis of MnO2 nanosheets on montmorillonite for oxidative degradation and adsorption of methylene blue. *J. Colloid Interface Sci.* **2018**, *510*, 207–220, doi:10.1016/j.jcis.2017.09.066.

8. Mekidiche, M.; Khaldi, K.; Nacer, A.; Boudjema, S.; Ameur, N.; Lerari-zinai, D.; Bachari, K.; Choukchou-braham, A. Organometallic modified montmorillonite application in the wastewater purification: Pollutant photodegradation and antibacterial efficiencies. *Appl. Surf. Sci.* **2021**, *569*, 151097, doi:10.1016/j.apsusc.2021.151097.

9. Xu, C.; Wu, H.; Gu, F.L. Efficient adsorption and photocatalytic degradation of Rhodamine B under visible light irradiation over BiOBr/montmorillonite composites. *J. Hazard. Mater.* **2014**, *275*, 185–192, doi:10.1016/j.jhazmat.2014.04.064.

10. Khataee, A.; Karaca, S.; Sheydaei, M. Artificial neural network modeling of photocatalytic removal of a disperse dye using synthesized of ZnO nanoparticles on montmorillonite. *Spectrochim. Acta Part A Mol. Biomol. Spectrosc.* **2015**, *140*, 465–473, doi:10.1016/j.saa.2014.12.100.

11. Xiang, H.; Tuo, B.; Tian, J.; Hu, K.; Wang, J.; Cheng, J. Preparation and photocatalytic properties of Bi-doped TiO 2 / montmorillonite composite. *Opt. Mater. (Amst).* **2021**, *117*, 111137, doi:10.1016/j.optmat.2021.111137.

12. Joseph, A.; Vellayan, K.; González, B.; Vicente, M.A.; Gil, A. Effective degradation of methylene blue in aqueous solution using Pd-supported Cu-doped Ti-pillared montmorillonite catalyst. *Appl. Clay Sci.* **2019**, *168*, 7–10, doi:10.1016/j.clay.2018.10.009.

13. Phyu, P.; Wang, J.; Thinn, T.; Wu, X.; Zhang, G. Fabrication of functionalized plasmonic Ag loaded Bi2O3/montmorillonite nanocomposites for efficient photocatalytic removal of antibiotics and organic dyes. *J. Alloys Compd.* **2020**, *818*, 152836, doi:10.1016/j.jallcom.2019.152836.

14. Khataee, A.; Sheydaei, M.; Hassani, A.; Taseidifar, M.; Karaca, S. Ultrasonics Sonochemistry Sonocatalytic removal of an organic dye using TiO2/Montmorillonite nanocomposite. *Ultrason. - Sonochemistry* **2015**, *22*, 404–411, doi:10.1016/j.ultsonch.2014.07.002.

15. Tao, E.; Xiao, X.; Yang, S. A new synthesizing method of TiO2 with montmorillonite: Effective photoelectron transfer to degrade Rhodamine B. *Sep. Purif. Technol.* **2021**, *258*, 118070, doi:10.1016/j.seppur.2020.118070.

16. Huang, Z.; Wu, P.; Gong, B.; Yang, S.; Li, H.; Zhu, Z.; Cui, L. Preservation of glutamic acid-iron chelate into montmorillonite to efficiently degrade Reactive Blue 19 in a Fenton system under sunlight irradiation at neutral pH. *Appl. Surf. Sci.* **2016**, *370*, 209–217, doi:10.1016/j.apsusc.2016.02.126.

17. Fatimah, I.; Purwiandono, G.; Hidayat, A.; Sagadevan, S.; Kamari, A. Mechanistic insight into the adsorption and photocatalytic activity of a magnetically separable γ-Fe2O3/Montmorillonite nanocomposite for rhodamine B removal. *Chem. Phys. Lett.* **2022**, *792*, 139410, doi:10.1016/j.cplett.2022.139410.

18. Natsir, M.; Putri, Y.I.; Wibowo, D.; Maulidiyah, M.; Salim, L.O.A.; Azis, T.; Bijang, C.M.; Mustapa, F.; Irwan, I.; Arham, Z.; et al. Effects of Ni–TiO2 Pillared Clay–Montmorillonite Composites for Photocatalytic Enhancement Against Reactive Orange Under Visible Light. *J. Inorg. Organomet. Polym. Mater.* **2021**, *31*, 3378–3388, doi:10.1007/s10904-021-01980-9.

19. Fatimah, I.; Wang, S.; Wulandari, D. ZnO/montmorillonite for photocatalytic and photochemical degradation of methylene blue. *Appl. Clay Sci.* **2011**, *53*, 553–560, doi:10.1016/j.clay.2011.05.001.

20. Peng, K.; Wang, H.; Li, X.; Wang, J.; Xu, L.; Gao, H.; Niu, M. One-step hydrothermal growth of MoS2 nanosheets/CdS nanoparticles heterostructures on montmorillonite for enhanced visible light photocatalytic activity. *Appl. Clay Sci.* **2019**, *175*, 86–93, doi:10.1016/j.clay.2019.04.007.

21. Amaly, N.; El-moghazy, A.Y.; Nitin, N.; Sun, G.; Pandey, P.K. Synergistic adsorption-photocatalytic degradation of tetracycline by microcrystalline cellulose composite aerogel dopped with montmorillonite hosted methylene blue. *Chem. Eng. J.* **2022**, *430*, 133077, doi:10.1016/j.cej.2021.133077.

22. Peng, A.; Wang, Y.; Yin, L.; Chen, Z.; Gu, C. Halide salts induced the photodegradation of a fat-burning compound 2,4-dinitrophenol by iron-montmorillonite. *Chemosphere* **2022**, *291*, 132694, doi:10.1016/j.chemosphere.2021.132694.

23. González, B.; Trujillano, R.; Vicente, M.A.; Rives, V.; Korili, S.A.; Gil, A. Photocatalytic degradation of trimethoprim on doped Ti-pillared montmorillonite. *Appl. Clay Sci.* **2019**, *167*, 43–49, doi:10.1016/j.clay.2018.10.006.

24. Peng, G.; Li, T.; Ai, B.; Yang, S.; Fu, J.; He, Q.; Yu, G. Highly efficient removal of enrofloxacin by magnetic montmorillonite via adsorption and persulfate oxidation. *Chem. Eng. J.* **2019**, *360*, 1119–1127, doi:10.1016/j.cej.2018.10.190.

25. Ye, P.; Lemley, A.T. Adsorption effect on the degradation of 4,6-o-dinitrocresol and p-nitrophenol in a montmorillonite clay slurry by AFT. *Water Res.* **2009**, *43*, 1303–1312, doi:10.1016/j.watres.2008.12.046.

26. Vidal, C.B.; André, B.; Ronaldo, F.; Bandosz, T.J. Reactive adsorption of pharmaceuticals on tin oxide pillared montmorillonite : Effect of visible light exposure. *Chem. Eng. J.* **2015**, *259*, 865–875, doi:10.1016/j.cej.2014.07.079.

27. Baizig, M.; Khalfallah, S.; Bassem, J.; Batis, N.; Trujillano, R. Preparation and Characterization of Different TiO2-Modified Montmorillonite Meso-Microporous Materials, with Enhanced Photocatalytic Activity. *Int. J. Eng. Res. Technol. (* **2015**, *4*, 182–192.